Journal of Materials Processing Technology 123 (2002) 13–17

Journal of Materials Processing Technology

www.elsevier.com/locate/jmatprotec

Grinding of alumina/aluminum composites

Zhaowei Zhong*, Nguyen Phu Hung

School of Mechanical and Production Engineering, Nanyang Technological University, Nanyang Avenue, Singapore 639798, Singapore

Received 29 October 2000

Abstract

With the anticipated widespread usage of metal matrix composites (MMCs) in the near future, the machinability of high performance MMCs needs to be understood. This paper reports research results obtained from the grinding of aluminum-based MMCs reinforced with Al_2O_3 particles using grinding wheels having SiC in a vitrified matrix and diamond in a resin-bonded matrix. The issues discussed are surface roughness, grinding force, type and size of the abrasives, grinding conditions, and the consequential sub-surface integrity. The study used grinding speeds of 1100–2200 m/min, a grinding depth of 15 μm for rough grinding and 1 μm for fine grinding, and cross-feeds of 3 and 1 mm for rough and fine grinding respectively, while maintaining a constant table feed-rate of 20.8 m/min. The surface integrity of the ground surfaces and sub-surfaces were analyzed using a scanning electron microscope (SEM) and a profilometer. The surface finish values, R_a, were scattered in the range 0.15–0.70 μm for the rough-ground samples, whilst a narrower range of 0.20–0.35 μm was achieved for the fine-ground samples. Smearing of aluminum on the ground surfaces was seen for rough grinding, but was negligible for fine grinding because all the Al_2O_3 particles of the ground surfaces were clearly visible when observed with the SEM. Grinding using a 3000-grit diamond wheel at depth of cut of 1 μm produced many ductile streaks on the Al_2O_3 particles. Both the Al_2O_3 particles and aluminum matrix were removed by micro machining. There were no cracks and defects found on the ground surfaces. There was almost no sub-surface damage, except for a rare cracked particle being found. Rough grinding with a SiC wheel followed by fine grinding with a fine-grit diamond wheel is recommended for the grinding of alumina/aluminum composites. © 2002 Published by Elsevier Science B.V.

Keywords: Metal matrix composites; Grinding; Ductile streaks

1. Introduction

Aluminum-based metal matrix composites (MMCs) reinforced with ceramic particles are known as advanced materials for their high specific strength, high wear resistance, and good damping characteristics. Methods to produce these composites and studies on their mechanical properties have gained popularity [1]. MMCs are primarily used in the astronautic, military and automobile industries. In addition, the sporting goods industry has also been in the forefront of MMCs development, capitalizing on the materials' high specific properties. There is also a growing interest in other industries, such as the shipping industry [2].

Reports on the machining of aluminum-based MMCs reinforced with ceramic particles [3–7] are still scarce. Despite many advantages, full implementation of MMCs is cost-prohibitive, partially due to the material's poor machinability. Although near-net shape MMC products can be manufactured, final finishing may still be needed for the final designed dimensions and required surface finish. A study on the machining of high performance MMCs, therefore, becomes important, especially where mass production is involved.

Sensitive cost and fabrication challenges including machining must be overcome for successful application of these composites. The surface finish and surface integrity are important for surface-sensitive parts subjected to fatigue or creep. Machine-induced sub-surface damage could have serious consequences. However, many machining methods often result in cracking, splintering and pulling-out of reinforcement particles. Sub-surface damage resulted from conventional and unconventional processes such as turning, drilling, milling, electrical discharge machining, abrasive jet machining, and laser machining [5]. A proper process such as grinding to obtain a good surface finish and damage-free surfaces is crucial for the application of the materials.

Ductile-mode machining of brittle materials, such as Al_2O_3 and SiC, has resulted in many innovative applications. It was reported that by having a critical depth of cut and with flattened grains slightly protruding from the surface of the grinding wheel, flawless machining, free of brittle fracture, is possible [8]. Evidence of plastic flow with Al_2O_3, Si_3N_4, and SiC was shown and a model based on the combination of two

* Corresponding author.
E-mail address: mzwzhong@ntu.edu.sg (Z. Zhong).

0924-0136/02/$ – see front matter © 2002 Published by Elsevier Science B.V.
PII: S0924-0136(02)00075-4

theories was proposed [9]. However, reports on the ductile-mode machining of aluminum-based MMCs reinforced with ceramic particles are still very scarce. Therefore, further studies on the ductile-mode machining of the materials are required.

This paper reports research results obtained from the grinding of aluminum-based MMCs reinforced with Al_2O_3 particles using grinding wheels having SiC in a vitrified matrix and diamond in a resin-bonded matrix. The issues discussed are surface roughness, grinding force, type and size of the abrasives, grinding conditions and the consequential sub-surface integrity.

2. Experiments

The MMCs chosen for the grinding experiments were 2618/Al_2O_3/10p (W2F10A) and 2618/$Al_2O_3$20p (W2F20A) detailed in Table 1. The grinding wheels used and grinding conditions are shown in Table 2. Six 2618/Al_2O_3/10p and six 2618/Al_2O_3/20p workpieces were milled to the same size. Three 2618/Al_2O_3/10p and three 2618/Al_2O_3/20p workpieces were rough-ground with an 80-grit vitrified-bond SiC grinding wheel at low, medium and high grinding speed. The remaining three pieces of 2618/Al_2O_3/10p and 2618/Al_2O_3/20p workpieces were first rough-ground with the SiC grinding wheel at low grinding speed, and then fine-ground with a 3000-grit resin-bonded diamond wheel at low, medium and high grinding speed.

Grinding experiments were carried out on an Okamoto precision surface-grinding machine (PSG-64DX). A Fuji inverter (FVR-G75) was attached to the machine so that the main spindle of the machine was capable of being changed. A dynamometer (Kistler9257A) was mounted on the table of the grinding machine to measure the grinding forces. The dynamometer was connected to charge amplifiers (Kistler5011) and the measured grinding forces were recorded using a chart recorder (Yokogawa LR8100). The grinding force reported here is the force perpendicular to a ground surface.

A SiC wheel mounted on a brake-controlled truing device and a single diamond dresser were used for truing the grinding wheels. SiC and WA dressing sticks were used for dressing the SiC and diamond grinding wheels, respectively. Dressing was carried out before every grinding experiment.

Table 2
Grinding wheels and grinding conditions for rough and fine grinding

	Rough grinding	Fine grinding
Grinding wheel		
Grain	Green SiC	Diamond
Grit size	80	3000
Bond	Vitrified-bond	Resin-bond
Diameter (mm)	350	350
Width (mm)	38	10
Dressing stick		
Grain	Green SiC	WA
Grit size	60	320
Grinding speed		
Low speed (m/min)	1100	1100
Medium speed (m/min)	1650	1650
High speed (m/min)	2200	2200
Depth of cut (μm)	15	1
Feed-rate (m/min)	20.8	20.8
Cross-feed (mm)	3	1

The surface roughness of the ground MMCs in the grinding (table feed) direction and cross-feed direction was measured using a Tokyo Seimitsu roughness tester. The cut-off was 0.8 mm and the evaluation length was 4 mm. The average value was calculated from three measured values in the same direction on each ground surface. The surface integrity of the ground surfaces was analyzed using a Cambridge–Leica scanning electron microscope (SEM). Furthermore, the ground surfaces were cleaned with alcohol, protected with epoxy, then sectioned with a diamond saw on a Buehler Isomet metallographic cutter. The specimens were cold vacuum mounted, ground, polished, and then etched in a solution of 2 ml HF (48%) + 3 ml concentrated HCl + 5 ml concentrated HNO_3 + 190 ml H_2O. Sub-surface damage was assessed by observing the etched samples using an SEM.

3. Results and discussion

The surface roughness values of rough and fine-ground MMCs are shown in Figs. 1 and 2, respectively. The values of the maximum grinding force measured during the rough and fine grinding experiments are shown in Figs. 3 and

Table 1
MMC workpieces used for the grinding experiments

Matrix	2618 Aluminum alloy
Reinforcement	10 vol.% Al_2O_3 particulate for 2618/Al_2O_3/10p (W2F10A); Al_2O_3 particle size: 9.3 μm 20 vol.% Al_2O_3 particulate for 2618/Al_2O_3/20p (W2F20A); Al_2O_3 particle size: 21 μm
Process	Direct extrusion with a flat face die Extrusion ratio 20:1 Billet temperature 420–430 °C Extrusion speed 3 m/min
Dimensions	19 mm (length) × 17 mm (width) × 17 mm (height)

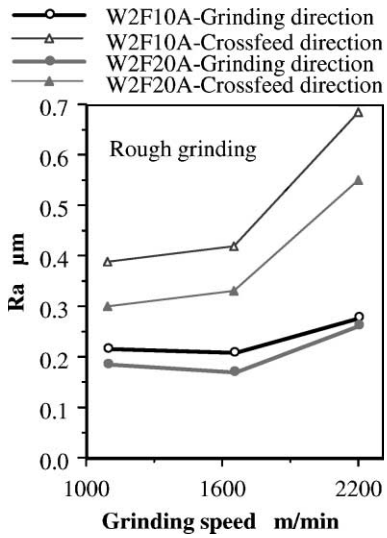

Fig. 1. Roughness values of ground MMC surfaces. Rough grinding (80-grit vitrified-bond SiC wheel; depth of cut: 15 μm; cross-feed: 3 mm; feed-rate: 20.8 m/min).

4, respectively. Figs. 5 and 6 show the top and the cross-section of the rough-ground surfaces, while Figs. 7, 8 and 9 show those of the fine-ground surfaces.

The roughness values of the rough-ground MMC surfaces in the cross-feed direction were higher than those in the grinding (table feed) direction. However, the effect of the measurement direction on the surface roughness values of the fine-ground MMC surfaces was not significant. The surface finish values, R_a, were scattered in the range of 0.15–0.70 μm for the rough-ground samples, whilst a narrower range of 0.20–0.35 μm was achieved for fine-ground samples. The surfaces ground by the 80-grit SiC wheel at speed of 1100 and 1650 m/min at a depth of cut of 15 μm

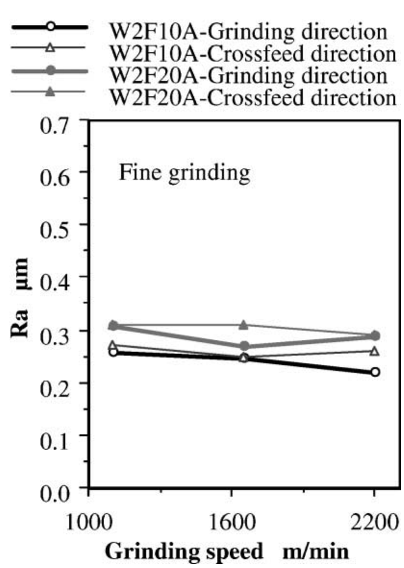

Fig. 2. Roughness values of ground MMC surfaces. Fine grinding (3000-grit resin-bond diamond wheel; depth of cut: 1 μm; cross-feed: 1 mm; feed-rate: 20.8 m/min).

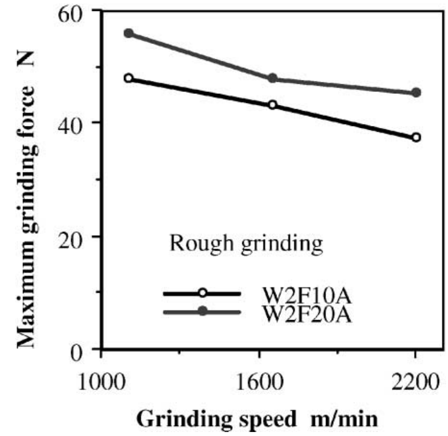

Fig. 3. Grinding forces for rough grinding (80-grit vitrified-bond SiC wheel; depth of cut: 15 μm; cross-feed: 3 mm; feed-rate: 20.8 m/min).

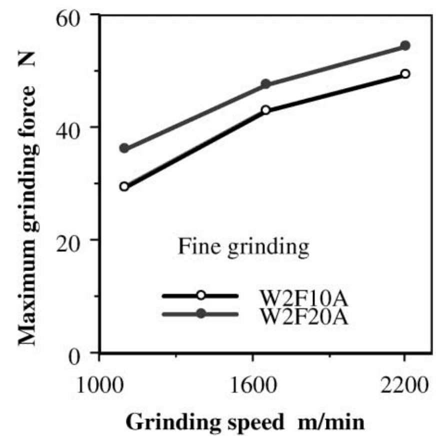

Fig. 4. Grinding forces for fine grinding (3000-grit resin-bond diamond wheel; depth of cut: 1 μm; cross-feed: 1 mm; feed-rate: 20.8 m/min).

had roughness values close to those of surfaces produced by the 3000-grit diamond grinding wheel at a depth of cut of 1 μm: this was due to the smearing of the aluminum matrix. Smearing of aluminum on the ground surfaces was seen for

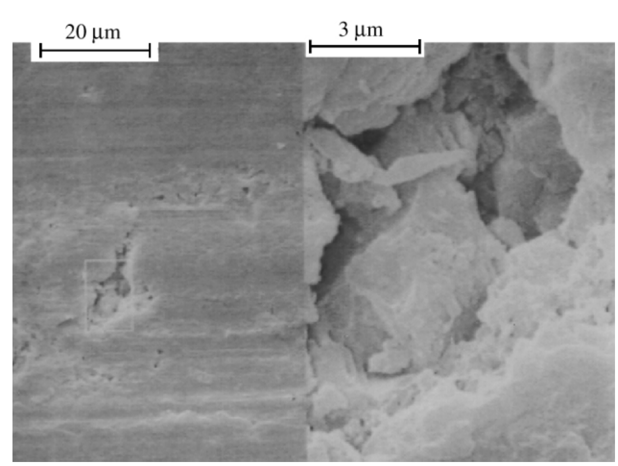

Fig. 5. An SEM micrograph of a ground MMC surface (2618/Al_2O_3/20p). Rough grinding (80-grit vitrified-bond SiC wheel; grinding speed: 2200 m/min; depth of cut: 15 μm, cross-feed: 3 mm; feed-rate: 20.8 m/min).

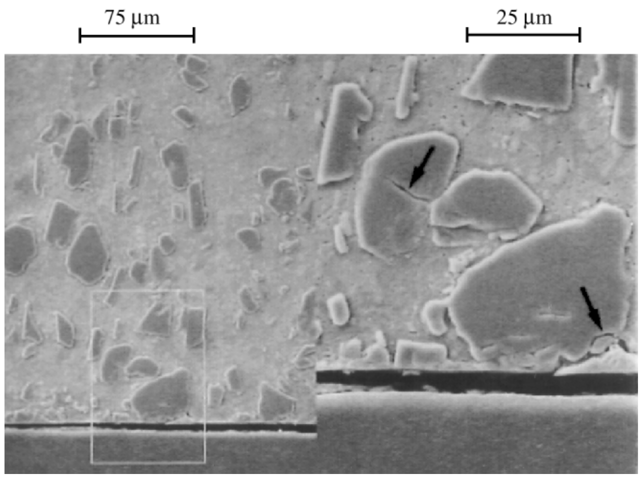

Fig. 6. Sub-surface of ground MMC (2618/Al_2O_3/20p). The arrows show commonly found cracks Al_2O_3 particles. Rough grinding (80-grit vitrified-bond SiC wheel; grinding speed: 2200 m/min; depth of cut: 15 μm; cross-feed: 3 mm; feed-rate: 20.8 m/min).

rough grinding, but was negligible for fine grinding because all the Al_2O_3 particles of the ground surfaces were clearly visible when observed with the SEM.

The maximum grinding force decreased with increasing grinding speed for the rough grinding, but increased with increasing grinding speed for the fine grinding. This could be due to the different abrasives, grit sizes and depths of cut used for the rough- and fine-grinding experiments, the thermally induced softened matrix at high speed for rough grinding, etc. For example, because the depth of cut was 15 μm for the rough grinding of Al_2O_3 particles (particle size: 9.3 or 21 μm), more heat was generated in the deformation zone. This softened the matrix at the higher grinding

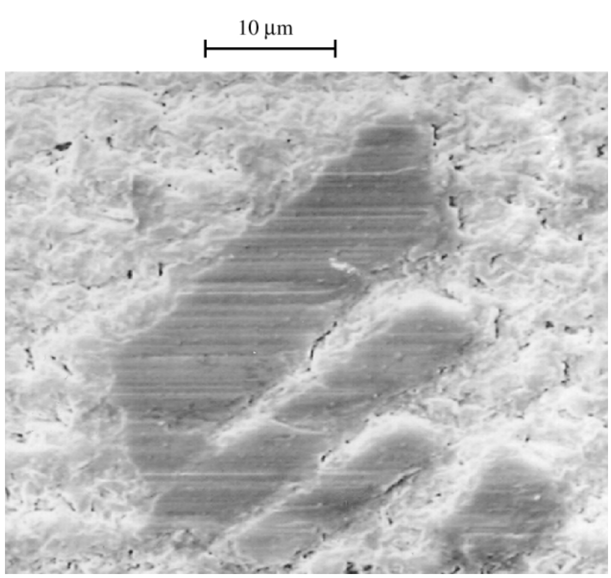

Fig. 7. SEM micrograph of ground MMC surface (2618/Al_2O_3/20p). Fine grinding (3000-grit resin-bond diamond wheel; grinding speed: 1100 m/min; depth of cut: 1 μm; cross-feed: 1 mm; feed-rate: 20.8 m/min).

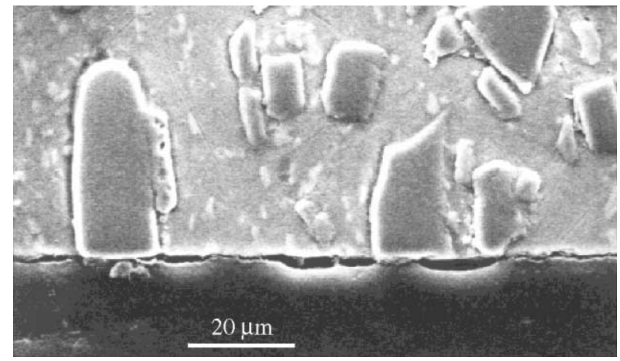

Fig. 8. Sub-surface of ground MMC (2618/Al_2O_3/20p). Fine grinding (3000-grit resin-bond diamond wheel; grinding speed: 1100 m/min; depth of cut: 1 μm; cross-feed: 1 mm; feed-rate: 20.8 m/min).

speed and reduced the grinding force component perpendicular to the ground surface. In the case of fine grinding, because the depth of cut was 1 μm, the thermal effect might be negligible. Further investigation is needed to better understand the micro machining mechanism of both the soft matrix and hard, brittle particles at the same time. However, from Figs. 3 and 4 it can be seen clearly that the grinding force required for grinding the MMCs with 20 vol.% Al_2O_3 particles is always higher than that for grinding the MMCs with 10 vol.% Al_2O_3 particles.

Figs. 5 and 6 show that cracks of the Al_2O_3 particles occur on and under the rough-ground surfaces. As mentioned above, the surfaces rough-ground at speed of 1100 and 1650 m/min have roughness values close to those of fine-ground surfaces. However, SEM pictures show that the surface topographies of the rough- and fine-ground surfaces with close surface roughness values are significantly different. No Al_2O_3 particles were seen on the rough-ground surfaces, except for some small holes showing fractured Al_2O_3 particles, as seen in Fig. 5. Almost the whole of the surfaces were smeared with the soft aluminum matrix.

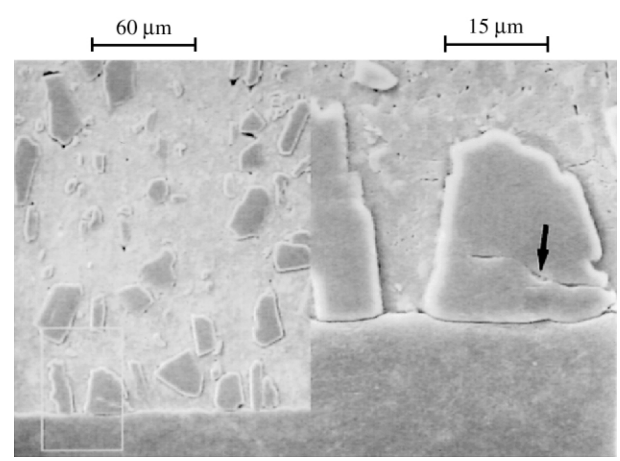

Fig. 9. The sub-surface of ground MMC (2618/Al_2O_3/20p). The arrow shows the very rare crack of an Al_2O_3 particle. Fine grinding (3000-grit resin-bond diamond wheel; grinding speed: 2200 m/min; depth of cut: 1 μm; cross-feed: 1 mm; feed-rate: 20.8 m/min).

Some of the aluminum chips were back-transferred on to the top of the surfaces.

SiC wheels are much cheaper than diamond wheels, the cost ratio being roughly 1:10–20. Because the depth of cut and cross-feed used were 15 and 3 times those for fine grinding respectively, the stock removal was substantial and the grinding time was much shorter as compared to that for fine grinding. Hence, the potential of using SiC wheels at least for rough grinding is high. Rough grinding parameters and dressing frequency should be optimized to make rough grinding using SiC wheels more attractive.

As shown in Fig. 7, grinding of the alumina/aluminum composite 2618/Al_2O_3/20p (20 vol.% Al_2O_3) using the fine-grit diamond wheel at 1 μm in-feed (depth of grinding) produced visible ductile streaks on the Al_2O_3 particles. Both the matrix and the Al_2O_3 particles were removed by micro machining because the ductile grinding marks were clearly seen on the Al_2O_3 particles. There were no cracks and defects found on the ground surfaces. There was almost no sub-surface damage as shown in Fig. 8, except for a very rare cracked particle, as shown in Fig. 9.

4. Summary of results

Grinding experiments using both 80-grit SiC in a vitrified matrix and 3000-grit diamond in a resin-bonded matrix were performed on aluminum-based MMCs reinforced with Al_2O_3 particles.

The surface finish values, R_a, were scattered in the range of 0.15–0.70 μm for the rough-ground samples, whilst a narrower range of 0.20–0.35 μm was achieved for fine-ground samples. Smearing of aluminum on the ground surfaces was seen in rough grinding, but was negligible for fine grinding because all the Al_2O_3 particles of the ground surfaces were clearly visible when observed with an SEM.

Grinding using the 3,000-grit diamond wheel at depth of cut of 1 μm produced many ductile streaks on the Al_2O_3 particles. Both the Al_2O_3 particles and aluminum matrix were removed by micro machining. There were no cracks and defects found on the ground surfaces. There was almost no sub-surface damage except for a rare cracked particle being found.

The potential of using SiC wheels at least for the rough grinding of alumina/aluminum composites is high, because SiC grains are harder than Al_2O_3 reinforcing particles and much less expensive than diamond grains. Rough grinding with a SiC wheel followed by fine grinding with a fine-grit diamond wheel is recommended for the grinding of alumina/aluminum composites.

References

[1] M.J. Tan, L.H. Koh, K.A. Khor, F.Y.C. Boey, Y. Murakoshi, T. Sano, J. Mater. Process. Technol. 37 (1993) 391–403.

[2] N.L. Loh, in: Proceedings of the International Symposium on High Performance Metal Matrix Composites, Japan, 1994, pp. 11–12.

[3] A.R. Chambers, S.E. Stephens, J. Mater. Sci. Eng. A 135 (1991) 287.

[4] L.A. Looney, J.M. Monaghan, P. O'Reilly, D.M.R. Taplin, J. Mater. Process. Technol. 33 (1992) 453.

[5] N.P. Hung, F.Y.C. Boey, K.A. Phua, H.F. Lee, J. Mater. Process. Technol. 56 (1996) 966–977.

[6] N.P. Hung, Z.W. Zhong, C.H. Zhong, in: Proceedings of the Fourth Conference on Composites Engineering, Hawaii, 1997, pp. 459–460.

[7] N.P. Hung, Z.W. Zhong, C.H. Zhong, J. Mater. Manuf. Process. 12 (6) (1997) 1075–1091.

[8] W. Konig, V. Sinhoff, SPIE, Lens and Optical Systems Design, 1992, pp. 778–788.

[9] K. Kitajima, G.Q. Cai, N. Kumagai, Y. Tanaka, H.W. Zheng, Ann. CIRP 41 (1) (1992) 367–371.